JOURNAL OF MATERIALS SCIENCE **39** (2004) 1213–1220

The influence of processing temperature on the structure and properties of mesophase-based polygranular graphites

F. FANJUL, M. GRANDA,*,‡ R. SANTAMARÍA, R. MENÉNDEZ
Instituto Nacional del Carbón, CSIC. Apartado 73, 33080-Oviedo, Spain
E-mail: mgranda@incar.csic.es

Two polygranular graphites were prepared by sintering a coal-tar pitch based mesophase and a naphthalene-based mesophase. The influence of temperature on the structural (density, porosity and light texture), mechanical (flexural strength) and electrical (electrical resistivity) properties of the carbons was studied at different stages of carbonization/graphitization (400–2600°C). The results show that the density of the materials increases continuously with temperature, pores mainly appearing below 800°C, during the low-sintering phase and at the initial stages of the solid-sintering process. Above this temperature, porosity decreases due to the densification of the materials. Densification is clearly evidenced by a reduction in interlayer spacing and an increase in crystallite size. Flexural strength and electrical resistivity follow a different trend depending on the temperature range. Thus, flexural strength reaches its maximum value at 1000°C, while electrical resistivity decreases continuously with temperature. Any variation in these properties is mainly related with porosity and crystallographic order. The different composition of the raw materials causes structural, mechanical and electrical changes to occur to different extent in both materials.

1. Introduction

Polygranular graphites are attractive materials for which applications are easily found in modern advanced technologies (e.g., nuclear reactor walls, electric discharge machines, special containers, semiconductors), where high chemical, mechanical, electrical and thermal performance is required [1, 2]. Such a useful combination of properties is a consequence of the peculiar structure of polygranular graphites. They are made up of very fine anisotropic local units (microcrystallites) that confer an isotropic behaviour on the whole material [1].

The traditional process of manufacturing polygranular graphites involves the use of granular premium petroleum coke as filler and coal-tar pitch as binder [1]. These two components are mixed, moulded, baked, impregnated and graphitized to give the final material. Impregnation and baking must be repeated several times to achieve adequate density and strength with the consequent economic implications. Moreover, in some applications, such as nuclear reactor walls, only high-purity graphites can be used. These limitations could be overcome by using high-purity precursors that allow high-density and high-strength materials to be obtained in one step. Carbonaceous mesophase is a self-sintering thermoplastic material, which by thermal treatment in an inert atmosphere (carbonization/graphitization) gives rise to polygranular graphites with optimum properties [1–8].

Structurally, carbonaceous mesophase is a discotic and nematic liquid crystal phase [9] formed as an intermediate during the carbonization of certain polycyclic aromatic hydrocarbons (PAH), either as single moieties or as a part of complex mixtures such as petroleum and coal-tar pitches [10]. The formation of the mesophase involves polymerization and condensation reactions, which lead to large planar and polyaromatic molecules (mesogens) [11]. Mobility and planarity are the most relevant characteristics of the mesogens because they establish the orientation and two-dimensional order necessary for the development of the structure of the subsequently formed graphitic layers [12]. Mesogens have the ability to associate, producing self-assembled stacks [13]. These stacks segregate in the form of small spheres (mesophase), which are optically anisotropic. At this stage, a biphasic system can be observed: (i) an isotropic phase made up of mesogens and (ii) mesophase. Mesophase grows by incorporating mesogens from the isotropic phase and by coalescence [13]. The mesophase spheres can be

*Author to whom all correspondence should be addressed.
‡*Present address*: Instituto Nacional del Carbón, CSIC, C/Francisco Pintado Fe, 26, 33011-Oviedo, Spain.

separated from the isotropic phase by the following procedures: solvent extraction [14, 15], high-temperature centrifugation [16, 17] and filtration under pressure at moderate temperatures [18].

The characteristics of the mesophase, which are directly related to the chemical composition and structure of the parent PAH, and operational conditions are critical for the final structure and properties of the polygranular graphite. During the carbonization and graphitization of the mesophase, different physico-chemical processes take place, leading to the formation of a graphitic material. These processes involve additional polymerization and condensation of the mesophase components, resulting in a rearrangement of the condensed molecules and the release of gases and volatiles. As a consequence, the material undergoes structural changes, such as volumetric contraction, development of porosity and an improvement in the crystalline order. The temperatures at which these changes may occur are of special importance because they determine the structure and properties of the graphite.

The aim of this work is to study the changes in the structure (porosity, light texture) and properties (flexural strength, electrical resistivity) of two polygranular graphites prepared from a coal-tar pitch based mesophase and a naphthalene-based mesophase at different stages of carbonization/graphitization.

2. Experimental

2.1. Materials used

Polygranular graphites were prepared from a coal-tar pitch based mesophase (M-A) and a naphthalene-based mesophase (M-B). M-A was obtained from an impregnating-grade coal-tar pitch by thermal treatment and subsequent hot filtration under pressure at laboratory scale. Thermal treatment was carried out at 430°C for 4 h. The thermally treated pitch, containing 32.3 vol% of mesophase, was then filtered in order to concentrate the mesophase. Filtration was carried out at 300–350°C with the aid of a nitrogen pressure of 0.5 MPa, using a 5 μm wire-cloth filter [18]. The resultant residue (M-A) contained 86.6 vol% of mesophase. M-B was a totally anisotropic commercial pitch produced by *Mitsubishi Gas Chemical Corporation*.

Prior to sintering, the mesophase samples were stabilized with air at 225°C, in the case of M-A (M-A225), and at 250°C, in the case of M-B (M-B250), using a multi-step temperature/time program described elsewhere in a previous work [19]. The main properties of the parent and stabilized mesophases are summarized in Table I.

TABLE I Characteristics of polygranular carbon precursors

Sample	C/H[a]	C/O[b]	TI[c]	NMPI[d]	I_{Ar}[e]
M-A	2.3	132	74.0	61.4	0.72
M-B	1.6	253	71.7	48.7	0.33
M-A225	2.4	42	90.8	69.3	0.78
M-B250	1.9	13	95.8	75.7	0.39

[a]Carbon/hydrogen atomic ratio.
[b]Carbon/oxygen atomic ratio.
[c]Toluene insolubles (wt%).
[d]1-methyl-2-pyrrolidinone insolubles (wt%).
[e]Aromaticity index, determined by FTIR.

2.2. Preparation of polygranular carbons

Stabilized mesophase samples (M-A225 and M-B250) were finely milled by means of a laboratory centrifugal ball mill, operating at 300 rpm for 30 min. The direction of rotation was reversed every one minute. ~15 g of sample was placed in a grinding jar, along with 30×10^{-6} m^3 of a dispersing agent (acetone/isopropanol: 50/50 vol%) to facilitate the milling of the sample. After milling, the powdered samples were moulded into prismatic specimens ($50 \times 10 \times 3$–4 mm) by applying a uniaxial mechanical pressure of 50 MPa at 140°C. The green materials were carbonized in a horizontal furnace according to the following multi-step temperature program: (i) at 1°C min^{-1} from room temperature up to 200°C; (ii) at 0.3°C min^{-1} from 200 up to 300°C; (iii) at 0.1°C min^{-1} from 300 up to 550°C; (iv) at 0.3°C min^{-1} from 550 up to 1000°C, the sample being maintained at this temperature for 30 min. In the case of the green material prepared with M-B250 the heating rate between 300 and 550°C was increased to 0.3°C min^{-1}. After carbonization, polygranular carbons were graphitized to 2600°C according to the following multi-step temperature/time program: (i) at 10°C min^{-1} from room temperature up to 950°C; (ii) at 2°C min^{-1} from 950 up to 1300°C, with a soaking time of 5 h; (iii) at 0.5°C min^{-1} from 1300 up to 1800°C, with a soaking time of 4 h; (iv) at 3°C min^{-1} from 1800 up to 2400°C, with a soaking time of 4 h; (v) at 1°C min^{-1} from 2400 up to 2600°C, with a soaking time of 1.5 h. Cooling was carried out at 1°C min^{-1}. Specimens at different stages of carbonization/graphitization were taken at 400, 550, 800, 1000, 1300, 1800, 2400 and 2600°C. Polygranular carbons from M-A225 were labelled as PC-A400, PC-A550, PC-A800, PC-A1000, PC-A1300, PC-A1800, PC-A2400 and PC-A2600 where the number refers to carbonization/graphitization temperature. Similarly polygranular carbons from M-B250 were labelled as PC-B400, PC-B550, PC-B800, PC-B1000, PC-B1300, PC-B1800, PC-B2400 and PC-B2600.

2.3. Characterization of polygranular carbons

The bulk density (d_b) was calculated by measuring the dimensions and weight of the specimens. Density in water (d_{H_2O}) was determined according to the ASTM C20 standard. Helium pycnometry was used for the determination of the density of the specimens in helium (d_{He}). Porosity accessible to water (P_{H_2O}) and porosity accessible to helium (P_{He}) were calculated from Equations 1 and 2, respectively:

$$P_{H_2O} = \left[1 - \left(d_b / d_{H_2O}\right)\right] \cdot 100 \quad (1)$$

$$P_{He} = \left[1 - (d_b / d_{He})\right] \cdot 100 \quad (2)$$

Reflected polarized light microscopy was performed on polished cross-sections of the polygranular carbons

embedded in epoxy resin, using a 1-λ retarder plate to generate interference colours.

X-ray diffraction was performed by using Cu K_α radiation ($\lambda = 0.154184$ nm) at a step size of 0.02° and a step time of 1 s between 5–90° 2θ. The mean interlayer spacing, d_{002}, and the crystallite size along the C-axis, L_c, were calculated from the peak position and half width of (002), using the Scherrer equation, the value of 0.90 being adopted for the constant 'k'.

Flexural strength was determined by a four-point-bending test, according to the ASTM C651 standard. Specimens of 40 × 8 × 3 mm were tested in a four-point rig over a span of 21 mm between 5-mm-diameter supported rollers. The load was applied by means of two 5-mm-diameter loading rollers separated 10 mm from one another. The machine cross-head speed was 1 mm min^{-1}. The results were quoted as the mean of values from 3 specimens of each material.

Electrical resistivity was measured at room temperature, using a laboratory-designed device. This device consists of two parallel copper plates (35 × 40 mm) connected to a power supply, which was allowed to operate to an intensity of 1 A. Prismatic specimens of 20×8×3 mm were fitted between the two copper plates. The voltage drop between two points of the specimens was measured by two pins separated 10 mm from one another and recorded on a multimeter. The electrical resistivity, quoted as the mean of 4 measurements on 3 specimens per sample, was calculated as follows (3):

$$\rho = (V \cdot s)/(I \cdot d) \quad (3)$$

where ρ, is the electrical resistivity (Ω m); V, the voltage (V); s, the cross-section of the specimen (m^2); I, the intensity (A); and d, the distance between the points of measurement (m).

3. Results and discussion

3.1. Composition and properties of polygranular carbon precursors

The coal-tar pitch based mesophase (M-A) is mainly made up of microspheres of a narrow size distribution (diameters between 10 and 30 μm), and to a lesser extent, of isotropic material (13.4 vol%), Fig. 1a. The naphthalene-based mesophase (M-B) is a totally anisotropic pitch, Fig. 1b. Both mesophases are mainly composed of carbon and hydrogen, especially in the case of M-B (Table I). The latter has a lower content of heteroatoms than M-A. The aromaticity index, determined by FTIR as being equivalent to the aromatic hydrogen/total hydrogen ratio [19], is much higher in M-A. The C/H ratio is also higher in M-A than in M-B. This indicates that the hydrogen in M-B is not only more abundant but also more aliphatic. The solubility parameters show that M-B is more soluble than M-A, especially in 1-methyl-2-pyrrolidinone (NMP), presumably due to the higher aliphatic hydrogen content of M-B (Table I).

When the mesophases are finely pulverized and moulded, the resultant specimens deform during subsequent sintering [9]. This is because the plasticity of the parent mesophases is excessively high. In order to reduce their plasticity, the mesophases were stabilized with air. Previous works [19] have shown that 225 and 250°C are the most appropriate stabilization temperatures for M-A and M-B, respectively. Under these conditions, a significant reduction in the plasticity of the mesophases takes place, while the self-adhesive properties of the samples are maintained, thereby allowing sintering but preventing further deformation [9]. The oxidative stabilization of the mesophases is a dehydrogenative process involving oxygen uptake and hydrogen consumption. The oxygen uptake and the hydrogen consumed are higher in the naphthalene-based mesophase (M-B250) than in the coal-tar pitch based mesophase (M-A225), as shown in Table I. This is because oxidative stabilization mainly occurs through the aliphatic hydrogen, which is more abundant in the naphthalene-based mesophase. Oxygen uptake gives rise to oxygen-containing functional groups (carbonyls, ethers, etc.) [19]. Most of these groups decompose during subsequent carbonization, with the release of CO and CO_2. Consequently, the release of such gases might be expected to be greater in M-B250 than in M-A225.

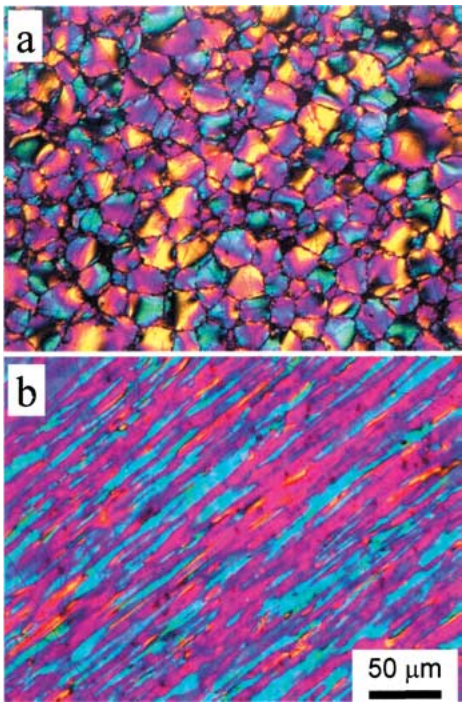

Figure 1 Light micrographs of (a) coal-tar pitch based mesophase and (b) naphthalene-based mesophase.

3.2. Structural and physical properties of polygranular carbons

The variation in the weight loss and volume shrinkage of the moulded mesophases with temperature is shown in Fig. 2. In general terms, the specimens from the coal-tar pitch based mesophase (PC-A series) lose more weight than the specimens from the naphthalene-based mesophase (PC-B series) over the entire range of temperatures. This weight loss occurs principally below 800°C. Two regions can be distinguished: (i) below 800°C and (ii) above 800°C. Weight loss by

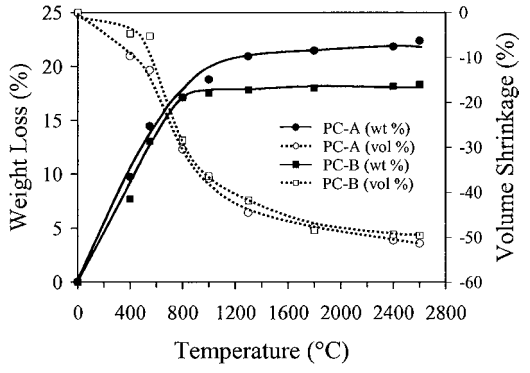

Figure 2 Variation in weight loss and volume shrinkage with temperature for the polygranular carbons.

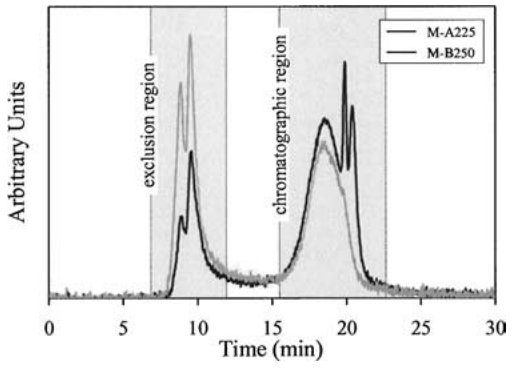

Figure 3 Size exclusion chromatograms of the 1-methyl-2-pyrrolidinone soluble fraction of the stabilized mesophases.

both materials is coincident at 800°C (17.1%), although at 400°C PC-A loses more weight than PC-B (9.7 and 7.7%, respectively). This indicates that the stabilized coal-tar pitch based mesophase has lower molecular weight compounds than the naphthalene-based mesophase. In fact, the size exclusion chromatograms of the 1-methyl-2-pyrrolidinone soluble fraction of the stabilized mesophases show that at the exclusion region, which contains large size compounds, the intensity of the M-B250 signal is higher than that of M-A225. Moreover, M-A225 also shows the presence of small size compounds at the chromatographic region (∼20–22 min), which are absent in M-B250 (Fig. 3).

Above 800°C, the weight loss undergone by the materials is very different. Between 800–1300°C, PC-A loses 3.8% of weight, whereas PC-B loses only 0.7%. This can be explained in terms of the removal of heteroatoms. After carbonization at 1000°C, PC-B is almost entirely composed of carbon (99.25%) [19], while PC-A1000 is made up of carbon and other heteroatoms such as nitrogen [19]. The removal of nitrogen between 800 and 1300°C [20–22] is presumably the factor mainly responsible for the higher weight loss in PC-A with respect to PC-B over this range of temperatures. Above 1300°C, both mesophases show a low weight loss, although materials from the coal-tar pitch based mesophase still lose more weight than materials from the naphthalene-based mesophase (1.4 and 0.5%, respectively).

Volume shrinkage is also more pronounced in the initial stages of carbonization (Fig. 2), especially between 550 and 1300°C. In this temperature range, the volume shrinks by 32 vol% in the coal-tar pitch based mesophase and by 37 vol% in the naphthalene-based mesophase. The shrinkage is considerable and takes place when the flow-sintering process has finished via the solid stage [4]. It is worth noting that shrinkage is not homogeneous in all directions. This is due to the effect of the uniaxial pressing applied during the moulding step. The materials shrink to a larger extent in the direction perpendicular to the application of pressure. However, above 800°C in the case of PC-A, and above 1000°C in the case of PC-B, shrinkage occurs predominantly in the pressing direction. This may be due to the fact that during pressing, the macromolecules (mesogens) of the mesophases are orientated by the effect of the pressure applied. In the subsequent carbonization up to 800–1000°C, shrinkage in the direction of the pressure applied is offset by the expansion produced by the gases. Above 800–1000°C when most of the gases have dispelled, the graphene planes contract, as a consequence of which shrinkage takes place preferentially in the pressing direction (Fig. 4). The increase in volume shrinkage above 1300°C is comparatively small and at 2600°C both materials have shrunk approximately by the same extent (∼50 vol%).

As a consequence of the variations in weight and volume, the density and porosity of the materials change significantly with temperature (Table II). Bulk density decreases slightly up to 550°C, and then increases sharply with the carbonization/graphitization temperature. The initial decrease in the bulk density of the materials is due to the fact that weight loss is more pronounced than volume shrinkage. At 550°C, the bulk

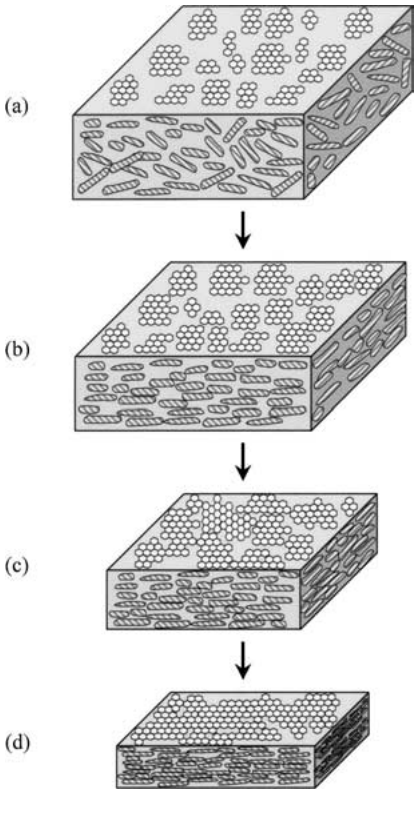

Figure 4 Schematic representation of the stacking of mesophase macromolecules: (a) before pressing, (b) after pressing, (c) after carbonization below 800°C and (d) after carbonization above 800°C.

TABLE II Density and porosity of polygranular carbons

Material	d_b [a]	d_{H_2O} [b]	d_{He} [c]	P_{H_2O} [d]	P_{He} [e]	ΔP [f]
PC-A	1100	–	1440	–	23.5	–
PC-A400	1100	1220	1460	9.8	23.8	14.0
PC-A550	1080	1210	1470	11.0	26.9	15.9
PC-A800	1310	1750	1860	25.2	29.5	4.3
PC-A1000	1420	1810	1980	21.2	28.0	6.8
PC-A1300	1500	1880	1990	20.6	24.6	4.0
PC-A1800	1550	1940	2050	20.4	24.8	4.4
PC-A2400	1590	1990	2110	20.3	24.7	4.4
PC-A2600	1600	2010	2120	20.4	24.7	4.3
PC-B	1150	–	1410	–	18.5	–
PC-B400	1140	1190	1420	4.7	20.3	15.6
PC-B550	1090	1180	1430	7.4	23.7	16.3
PC-B800	1360	1600	1790	14.9	24.1	9.2
PC-B1000	1470	1700	1820	13.4	19.2	5.8
PC-B1300	1570	1720	1930	8.4	18.2	9.8
PC-B1800	1640	1800	2040	8.6	19.4	9.8
PC-B2400	1690	1830	2070	7.4	18.3	10.9
PC-B2600	1710	1840	2090	7.0	18.0	11.0

[a]Bulk density (kg m^{-3}).
[b]Density in water (kg m^{-3}).
[c]Density in helium (kg m^{-3}).
[d]Porosity accessible to water (vol%).
[e]Porosity accessible to helium (vol%).
[f]Difference between P_{He} and P_{H_2O}.

density of both materials is similar (∼1100 kg m^{-3}), but above this temperature, densification occurs to a larger extent in PC-B than in PC-A (56 and 48%, respectively). This is because PC-A has a 13.4 vol% of isotropic phase, which is less dense than the anisotropic phase [23]. Assuming that densification in PC-A is an effect that is mainly associated with the anisotropic phase, shrinkage up to 2600°C might be expected to be around 55 vol% whereas the bulk density of the polygranular graphite ought to be similar to that prepared with PC-B (1700 kg m^{-3}).

The densities in water follow the same trend as the bulk densities (Table II). In contrast, the helium densities increase continuously with the carbonization/graphitization temperature, especially in the temperature range between 550 and 800°C (Table II).

The development of porosity is related to these changes in density. It is not surprising, therefore, that the highest development in porosity occurs between 550 and 800°C (Table II). Pores accessible to helium (P_{He}) and pores accessible to water (P_{H_2O}) were determined from the bulk-helium densities and bulk-water densities, respectively. The most important changes are observed in P_{H_2O}. In both materials, P_{He} increases slightly to 800°C, decreasing between 800 and 1300°C, then remaining almost constant up to 2600°C. P_{H_2O} follows a similar trend, although, it doubles its value between 550 and 800°C (Table II). These results show that the formation of pores accessible to water begins during the flow-sintering process, but it is in the initial stages of the solid-sintering process (550–800°C) that these pores are massively formed.

The values of P_{He} and P_{H_2O} give an approximate idea of the type of pores formed. Of course, all the pores accessible to water are also accessible to helium. However, the pores accessible to helium may not be accessible to water. The difference between P_{He} and P_{H_2O} (ΔP), therefore, allows changes in the size of the pores to be estimated. These changes are particularly significant in the 550–850°C temperature range. Thus, ΔP at 550°C is 15.9 and 16.3 for polygranular carbons from PC-A and PC-B, respectively. At 800°C, ΔP decreases to 4.3 and 9.2 for polygranular carbons from PC-A and PC-B, respectively. These changes suggest that pores initially accessible to helium but not to water are transformed into pores accessible to both helium and water. This might be due to the fact that gases eliminated at this stage of the carbonization (i.e., H_2, CH_4, CO and CO_2) [4] erode the small-size pores, giving rise to larger pores that presumably form an interconnected network. Once the pores are eroded and interconnected, the gases are freely evacuated and changes in P_{He} and P_{H_2O} become less relevant.

3.3. Microstructure of polygranular carbons

Polarized-light microscopy provides valuable information about the microstructural changes involved during the carbonization/graphitization of the polygranular carbons. The formation of pores begins at the early stages of carbonization. At 400°C pores of different sizes can be observed in both materials, especially in those derived from the PC-B mesophase. PC-B400 shows spherical pores of about 5–20 μm (Fig. 5d, position A). These pores are formed during the initial stages of the flow-sintering process due to the release of gases and volatiles. Such pores are not present in the green material (Fig. 5b). It is worth noting that pores in PC-A400 (Fig. 5c) are smaller in size than in PC-B400, even though in the former material P_{He} and P_{H_2O} are larger than in PC-B400. At 800°C pores become larger and more irregular in shape (Fig. 6). PC-B800 exhibits pores of about 40 μm (Fig. 6b, position A). A distinctive feature distinguishing materials derived from PC-A and PC-B, apart from the size of the pores, is that in the former the isotropic phase remains as isotropic as it was during carbonization, the larger-size pores being mainly associated with particles that contain this phase (Fig. 6a, position B). This might be due to the fact that the isotropic phase is more plastic and softens at a lower temperature than the mesophase [23]. With increasing temperature, the number of pores observed under the polarized-light microscope remains almost constant. However, there is a slight decrease in size (Fig. 6c, d, e and f), which is in agreement with the volume shrinkage to be expected in materials with increasing temperature (Fig. 2).

From these results, it can be inferred that pores are more numerous and smaller in size in PC-A series than in the PC-B series. This facilitates the description of possible mechanisms of sintering for both mesophases. Fig. 7 displays one possible model of the sintering process. As the individual particles shrink in unison during carbonization, high-efficiency sintering occurs, and consequently, bulk shrinkage is uniform. Low porosity can be expected in this case (Fig. 7b). In contrast, when the particles shrink independently and/or locally there is poor sintering, and consequently, bulk shrinkage is

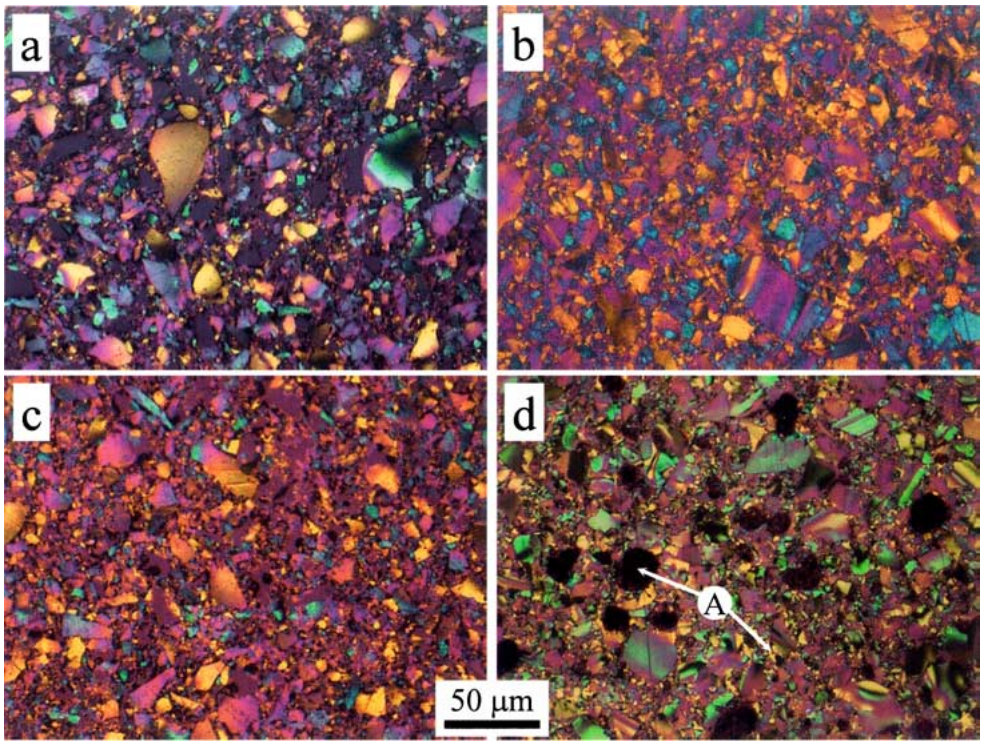

Figure 5 Light micrographs of (a) green material PC-A, (b) green material PC-B, (c) PC-A400 and (d) PC-B400.

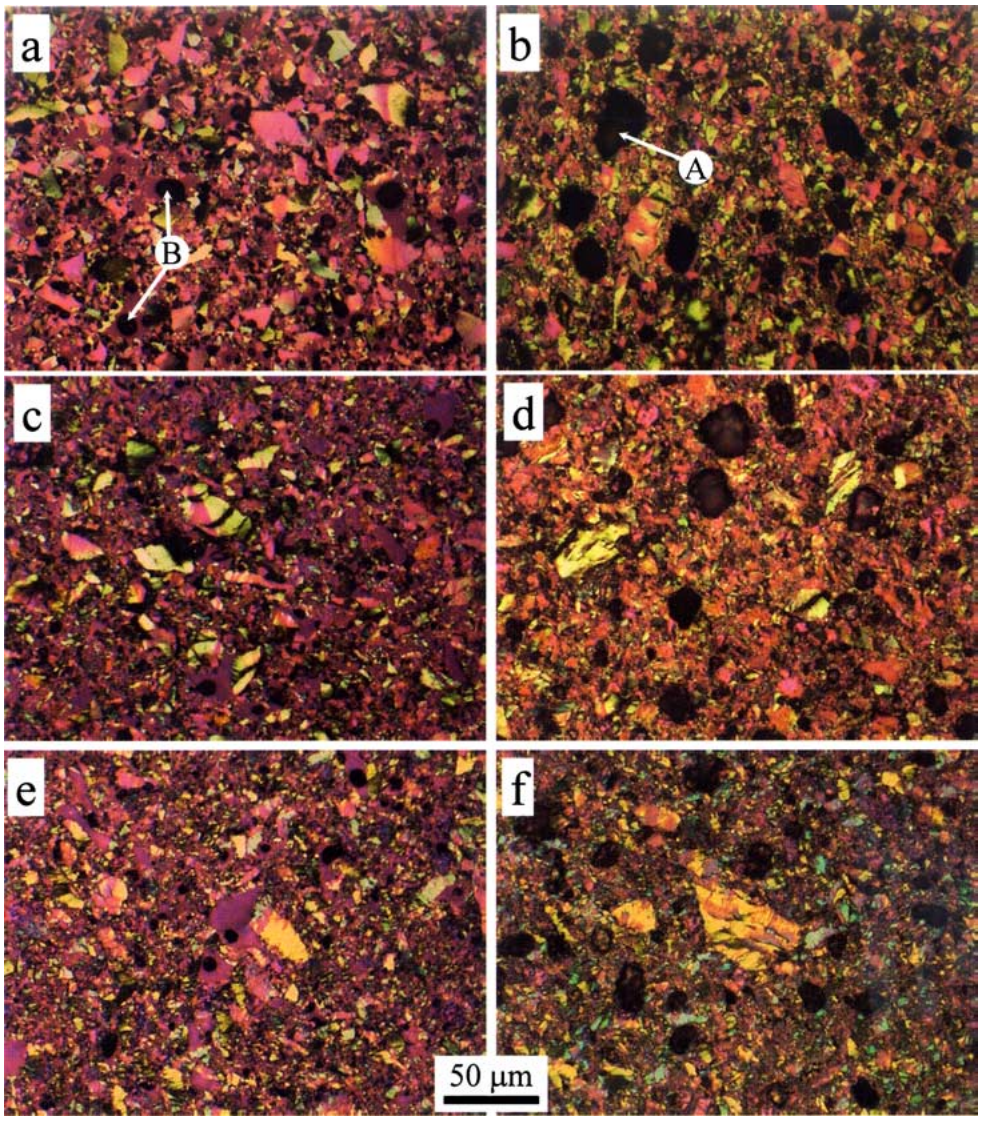

Figure 6 Light micrographs of (a) PC-A800, (b) PC-B800, (c) PC-A1800, (d) PC-B1800, (e) PC-A2600 and (f) PC-B2600.

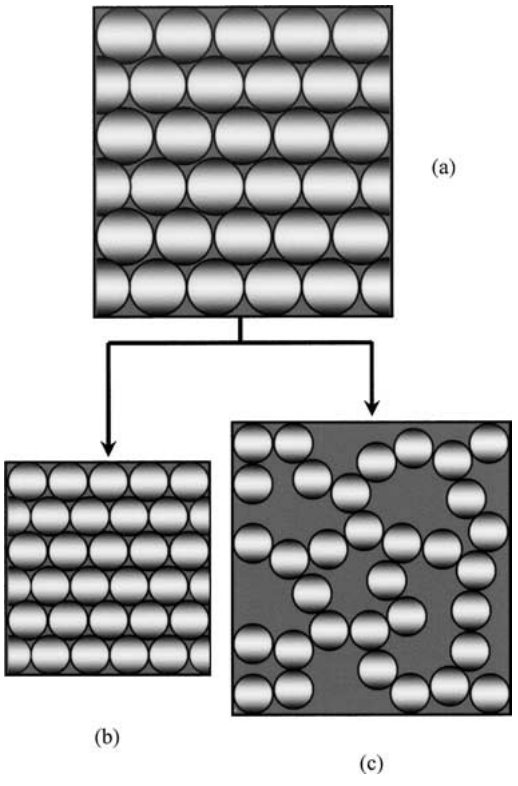

Figure 7 Schematic model of the sintering process: (a) packed green material, (b) high-efficiency sintering and (c) low-efficiency sintering.

non-uniform. In this case, many inter-particle pores may form (Fig. 7c), the development of which might be expected to increase the porosity of the sintered materials substantially. PC-A and PC-B show an intermediate behaviour. However, the larger amount of pores in PC-A suggests that this mesophase tends to behave more in accordance with the second model (Fig. 7c) than the PC-B mesophase.

3.4. Crystallographic parameters of polygranular carbons

The crystallographic parameters follow the same trend in both materials (Table III). PC-A1000 and PC-B1000 show the same mean interlayer spacing (d_{002}) and a similar crystallite size along the *c*-axes (L_c). The most significant peaks in the diffractograms are those at (002), corresponding to the basal plane reflection at a 2θ angle of about 26°, (100) at about 42° and (004) at about 54°. In the temperature range between 1000 and 1800°C d_{002} decreases down to 0.344 nm (turbostratic carbon) [21] whereas L_c increases up to ~10 nm. In these temperature ranges peaks can be seen at about 44° (101), 60° (103), 77° (110), 83° (112) and 87° (006), as well as at the temperatures mentioned above. These diffraction patterns show that a three-dimensional order is obtained after graphitization at 2600°C. However, when the diffraction patterns of polygranular graphites from mesophase PC-A and mesophase PC-B are compared, PC-B2600 shows a higher intensity than PC-A2600. This might be due to the presence of isotropic material in PC-A2600, which does not contribute to the intensity of the X-ray diffraction pattern.

TABLE III Crystallographic parameters of polygranular carbons

Material	d_{002} [a]	L_c [b]	L_a [c]
PC-A1000	0.353	1.99	–
PC-A1300	0.351	2.45	–
PC-A1800	0.344	9.73	25.95
PC-A2400	0.339	20.25	45.08
PC-A2600	0.338	24.19	47.09
PC-B1000	0.353	2.05	–
PC-B1300	0.349	3.39	–
PC-B1800	0.344	10.15	28.18
PC-B2400	0.339	20.60	47.46
PC-B2600	0.338	22.11	50.90

[a]Mean interlayer spacing (002), nm.
[b]Crystallite size along *c*-axes (002), nm.
[c]Crystallite size along *a*-axes (110), nm.

3.5. Mechanical and electrical properties of polygranular carbons

The evolution of the mechanical and electrical properties of the polygranular carbons is merely a consequence of the structural changes involved during their carbonization/graphitization. In this respect, porosity and sintering efficiency has a significant influence on the properties of the materials. It is not surprising, therefore, that polygranular carbons derived from PC-B mesophase exhibit higher flexural strength (Fig. 8a) and lower electrical resistivity (Fig. 8b) than polygranular carbons derived from PC-A mesophase.

Below 800°C, the materials show poor mechanical behaviour, although between 550 and 800°C, once the flow-sintering process has been concluded, there is a significant improvement in flexural strength. Above

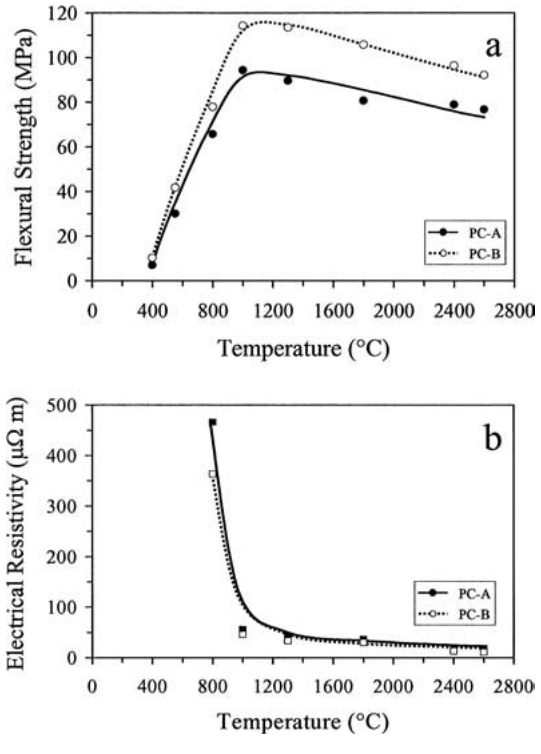

Figure 8 Variation in (a) flexural strength and (b) electrical resistivity with temperature for polygranular carbons obtained from mesophase PC-A and mesophase PC-B.

800°C, flexural strength increases until a maximum value at 1000°C is reached. This is coincident with the beginning of the decrease in porosity (Table II). At temperatures above 1000°C flexural strength decreases slightly. The same behaviour has also been found by other authors [2], who attributed the decrease in flexural strength to the graphitization of the materials. Graphitization causes a reduction in interlayer spacing (Table III), favouring the shear stresses that produce delamination of the materials.

The electrical resistivity of the polygranular carbons decreases with increasing temperature (Fig. 8b). Below 800°C, the materials do not conduct electricity. Above this temperature electrical resistivity falls. Unlike flexural strength, the electrical properties of the materials improve with graphitization. The growth of crystallite units and the reduction in interlaminar spacing (Table III) favours the passing of current, thereby reducing electrical resistivity.

4. Conclusions

The chemical composition of the mesophase precursor of polygranular carbons determines the differences in weight loss and volume shrinkage during the carbonization/graphitization processes. The materials from coal-tar pitch based mesophase (PC-A) lose more weight than the materials from naphthalene-based mesophase (PC-B). However, differences in volume shrinkage are less pronounced. As a result, the materials from mesophase PC-B show higher values of density and lower values of porosity.

In general terms, the development of porosity occurs below 800°C. Above this temperature, the volume of porosity and the size of the pores remain almost constant or even decrease. The materials from mesophase PC-A develop more porosity, but the pores are smaller in size. Moreover, the largest pores in these materials are mainly associated with residual isotropic material.

Despite the different nature and behaviour of the mesophases during carbonization/graphitization, the values of the crystallographic parameters show that the three-dimensional order achieved after graphitization at 2600°C is similar in both materials.

The materials prepared from naphthalene-based mesophase show higher flexural strength and lower electrical resistivity than the materials from coal-tar pitch based mesophase at any of the temperatures studied. However, differences in electrical resistivity are less significant. This is because in this type of material flexural strength is a property that is mainly governed by porosity and sinterability, whereas electrical resistivity is mainly dependent on porosity, sinterability and crystallographic order.

Acknowledgements

The authors would like to thank CICYT-FEDER (Project Ref. 1FD1997-1657MAT) for financial support.

References

1. A. OYA, "Introduction to Carbon Technologies" (Publicaciones de la Universidad de Alicante, Alicante, 1997) p. 564.
2. B. RAND and R. WOLF, "Design and Control of Structure of Advanced Carbon Materials for Enhanced Performance" (Kluwer Academic Publishers, Dordrecht, 2001) p. 241.
3. I. MOCHIDA, R. FUJIURA, T. KOJIMA, H. SAKAMOTO and F. KANNO, *Carbon* **32** (1994) 961.
4. W. R. HOFFMANN and K. J. HÜTTINGER, *ibid.* **32** (1994) 1087.
5. G. BATHIA, R. K. AGGARWAL, N. PUNJABI and O. P. BAHL, *J. Mater. Sci.* **32** (1997) 135.
6. J. SCHMIDT, K.D. MOERGENTHALER, K. P. BREHLER and J. ARNDT, *Carbon* **36** (1998) 1079.
7. M. MARTÍNEZ-ESCANDEL, P. CARREIRA, M. A. RODRÍGUEZ-VALERO and F. RODRÍGUEZ-REINOSO, *ibid.* **37** (1999) 1662.
8. F. FANJUL, M. GRANDA, R. SANTAMARÍA and R. MENÉNDEZ, *J. Mater. Sci.* **38** (2003) 427.
9. J. D. BROOKS and G. H. TAYLOR, *Nature* **206** (1965) 697.
10. J. D. BROOKS and G. H. TAYLOR, "Chemistry and Physics of Carbon" (Marcel Dekker Inc., New York, 1968) p. 243.
11. L. GHERGHEL, C. KÜBEL, G. LIESER, H. J. RÄDER and K. MÜLLEN, *JACS* **124** (2002) 13130.
12. R. HURT, G. KRAMMER, G. CRAWFORD, K. Q. JIAN and D. C. RULISON, *Chem. Mater.* **14** (2002) 4558.
13. H. MARSH and M. A. DÍEZ, "Liquid Crystalline and Mesomorphic Polymers" (Springer-Verlag, New York, 1994) p. 231.
14. A. GSCHWINDT and K. J. HÜTTINGER, *Carbon* **32** (1994) 1105.
15. Y. G. WANG, Y. C. CHANG, S. ISHIDA, Y. KORAI and I. MOCHIDA, *ibid.* **37** (1999) 969.
16. L. S. SINGER, D. M. RIFFLE and A. R. CHERRY, *ibid.* **25** (1987) 249.
17. M. KODAMA, T. FUJIRUA, K. ESUMI, K. MEGURO and H. HONDA, *ibid.* 26 (1988) 595.
18. C. BLANCO, R. SANTAMARÍA, J. BERMEJO and R. MENÉNDEZ, *ibid.* **35** (1997) 1191.
19. F. FANJUL, M. GRANDA, R. SANTAMARÍA and R. MENÉNDEZ, *Fuel* **81** (2002) 2061.
20. A. OBERLIN, "Chemistry and Physics of Carbon" (Marcel Dekker Inc., New York, 1989) p. 65.
21. M. BRAUN and K. J. HÜTTINGER, *Carbon* **34** (1996) 1473.
22. J. MACHNIKOWSKI and L. WAJZER, *Fuel* **73** (1994), 957.
23. C. BLANCO, R. SANTAMARÍA, J. BERMEJO and R. MENÉNDEZ, *Carbon* **38** (2000) 1169.

Received 12 May
and accepted 7 October 2003